

Received May 27, 2021; reviewed; accepted August 03, 2021

DFT and TOF-SIMS study of the interaction between hydrogen sulfide ion and malachite (-201) surface

Yingbo Mao ^{1,2}, Dandan Wu ¹, Lingyun Huang ¹

¹ State Key Laboratory of Complex Nonferrous Metal Resources Clean Utilization, Kunming University of Science and Technology, Kunming 650093, PR China

² Faculty of Science, Honghe University, Mengzi 661100, PR China

Corresponding authors: wdd1006530@sina.com (Dandan Wu), 12607199@qq.com (Lingyun Huang)

Abstract: In this paper, the mechanism of interaction between hydrogen sulfide ions and malachite was investigated using density functional theory (DFT) calculations and time of flight secondary ion mass spectrometry (TOF-SIMS). The DFT calculations showed that HS⁻ adsorption on the malachite (-201) surface was stronger than that of S adsorption resulting from the higher number of electron transfers in the solution which accelerated the sulfidation reaction rate. Density of states (DOS) analysis showed that the near Fermi level was jointly contributed to by the Cu 3d, O 2p, O 2s, and S 3p orbits after adsorption of HS⁻ on the malachite (-201) surface. It was found that the 2p orbital of O and the 3p orbital of S overlapped, indicating that S not only reacted with Cu, but also with O. The TOF-SIMS detected S⁻ and CuS₂⁻ fragment ion peaks in the 0–150 m/z negative segment of mass spectra. TOF-SIMS also showed that copper sulfide films of certain thicknesses were formed, demonstrating the effectiveness of hydrogen sulfide sulfidation in flotation processes.

Keywords: malachite, hydrogen sulfide ions, sulfidation, DFT, TOF-SIMS

1. Introduction

Copper is a non-ferrous metal that is highly integrated into to human being's lives. (Liu et al., 2016; Yin et al., 2019). It is widely used in the electronics, light, construction, and national defense industries, as well as machinery manufacturing and other fields (Feng et al., 2017). Copper is the second most consumed non-ferrous metal material in China, the first being aluminum. Copper is mainly extracted from its sulfide, which has driven the excessive exploitation and utilization of copper sulfide resources as the demand for copper has increased. Based on current trends, the over exploitation of oxidized copper resources appears inevitable (Feng et al., 2018a; Huang et al., 2016; Liu et al., 2019; Liu et al., 2018; Shen et al., 2019). Oxidized copper minerals make up important proportions of copper resources, among which malachite represents one of the most important oxidized copper minerals (Li et al., 2019). In general, it is difficult to use a conventional collector for the direct flotation of oxidized copper ore owing to its hydroxylation and solubility due to its surface characteristics (Feng et al., 2018b). Because of this, oxidized copper ore usually needs to be sulfidized to expose the copper and sulfide compounds at the surface of the mineral, ultimately increasing their floatability.

The sulfidation xanthate flotation method is commonly used to recover copper from oxidized copper minerals (Corin et al., 2017; Kalichini et al., 2017; Lee et al., 2009; Marion et al., 2017; Zhou and Chander, 1993). The common sulfidizing reagents include sodium sulfide (Na₂S), sodium hydrogen sulfide (NaHS), and ammonium sulfide [(NH₄)₂S] (Kongolo et al., 2003; Lee et al., 1998; Park et al., 2016). The purpose of the sulfidation process is to change the malachite surface into a sulfide surface, which increases the floatability of the mineral (Cao et al., 2009). This process includes the dissolution of sodium sulfide in an aqueous suspension as sulfide ions and hydrogen sulfide ions; the absorption of sulfide ions and hydrogen sulfide ions at the malachite surface; the chemical and/or electrochemical reactions

at the malachite surface in the CuS form; and the possible dissolution of some surface species. It should be pointed out that sulfidation of the malachite surface has some shortcomings. The effect of sulfidation depends largely on the amount of sulfidizing agent used. However, this is difficult to control in industrial production, and the use of excessive sulfidizing dosages usually leads to poor flotation performance. This is because excess sulfidizing agents form colloidal copper sulfur species in the pulp solution, which hinders the adsorption of xanthate on the mineral surface (Castro et al., 1974a; Castro et al., 1974b).

Considering the distribution the various coefficients in the Na₂S solution, which is a function of pH, H₂S will be the dominant species when pH < 7.0, whereas HS⁻ will dominate when pH > 7.0 and S²⁻ when pH > 13.9 (Ejtemaei et al., 2014; Gush, 2005; Malghan, 1986). The optimal pH of the sulfidation flotation method for the recovery malachite is approximately 9.5. Because this is the pH range wherein HS⁻ dominates, HS⁻ likely has an important role in flotation. Accordingly, it is likely that HS⁻ species interact with metallic ions on the mineral surface and generate a sulfidized surface film that facilitates the flotation of the oxide minerals (Bessiere et al., 1991). However, this needs to be better understood, so it is of great significance to study the sulfidation of malachite by hydrogen sulfide ions.

DFT is a method to study the electronic structure of multi-electron systems. DFT calculation is widely used to explore mineral crystal structure, mineral surface properties, and adsorption of agent molecules on mineral surfaces (Chen et al., 2018). TOF-SIMS provides elemental, chemical state, and molecular information of surfaces of solid materials. TOF-SIMS instrument provides a unique 3D analysis capability. The information TOF-SIMS provides about surface layers or thin film structures is important for many industrial and research applications where surface or thin film composition plays a critical role in performance (Lai et al., 2021).

In this study, based on the electronic geometry and atomic surface properties of malachite (-201) crystals, we applied density functional theory (DFT) calculations to the flotation research field. The DFT method was used in the present study to simulate the interactions between the surface of malachite (-201) and HS⁻. The adsorption of hydrogen sulfide ions on the malachite (-201) surface was investigated using time of flight secondary ion mass spectrometry (TOF-SIMS).

2. Materials and methods

2.1. Computational details

The simulated calculations were conducted in the CASTEP module of Materials Studio (MS) (Clark et al., 2005). In the calculations, the commutative correlation function is described by the PW91 gradient correction function under the general gradient approximation (GGA). The Ultrasoft of PW91 group is used to describe the interaction between ion cores and valence electrons (Perdew et al., 1986; Perdew et al., 1992; Perdew and Wang, 1992; Perdew et al., 1996). Valence electrons were selected for the calculation of the pseudopotential of each atom, including Cu 3d¹⁰ 4s¹, C 2s² 2p², O 2s² 2p⁴, H 1s¹, and S 3s² 3p⁴. Based on the experimental results, it was appropriate to set the cut-off energy at 351 eV. In the self-consistent field operation, the Pulay density mixing method was adopted, and its convergence precision was set to 2.0 × 10⁻⁵ eV atom⁻¹. The BFGS algorithm was adopted to optimize the model structure, and the convergence standard of optimization parameters, including interactions among atoms, was set to 0.005 eV nm⁻¹. The convergence standard of internal stress in the crystal was set at 0.1 GPa. The maximum atomic displacement convergence standard was set at 0.002 Å.

The sulfidation of malachite was investigated to analyze the HS⁻ adsorption configuration and HS⁻ adsorption energy on the malachite (-201) surface. The adsorption energy (ΔE_{ads}) of HS⁻ adsorbed on the malachite (-201) surface was calculated as follows:

$$\Delta E_{ads} = E_{malachite+x} - E_{malachite} - E_x \quad (1)$$

where ΔE_{ads} refers to the adsorption energy of the malachite (-201), $E_{malachite+x}$ refers to the total energy of the malachite (-201) surface with HS⁻ adsorption; $E_{malachite}$ refers to the total energy of the malachite (-201) surface; and E_x refers to the energy of HS⁻. A negative ΔE_{ads} signifies that the reaction can occur spontaneously, and the more negative the value is, the more likely the adsorption reaction is to occur and the stronger the adsorption. Since density function simulation calculations are carried out

in vacuum, the adsorption energy calculated varies among different calculation systems. They do not represent the actual energies, and the adsorption energy results only provide a qualitative basis.

2.2. TOF-SIMS

TOF-SIMS is a measurement technique used to determine the mass of ions by exciting the surfaces of samples with primary ions and emitting extremely small amounts of secondary ions. The different masses are calculated according to the time it takes the secondary ions to fly to the detector. It can detect concentrations at the PPM scale or smaller and facilitates deep analysis of a mineral's interior. Pure malachite samples were procured from Yunnan Province, China. The rectangularly-shaped samples ($1 \times 1 \times 0.3$ cm) were polished with wet silicon carbide paper sequentially from 220, 400, 600, 1000, 2000, and 4000 grit, and then polished using flannelette with a 2.5 μm diamond spray. Sample (a) was malachite + DI water and sample (b) was malachite + hydrogen sulfide ions. The reaction times of the above reagent combinations were all 10 minutes. The TOF-SIMS test conditions are shown in Table 1.

Table 1. Test conditions of TOF-SIMS

Ion Mass Analysis		depth/3D Profiling	
primary ion	Bi_3^+	sputter ion	Cs^+
primary ion energy	15kV	sputter energy	2kV
analysis current	0.47pA	sputter current	157.05nA
analysis area	500×500 μm^2 (for surface)	sputter area	300×300 μm^2
	100×100 μm^2 (for depth/3D Profiling)		
measurement time	75s (for surface)	sputter time	245s
	311s (for depth/3D Profiling)		
mode	Spectrometry	sputter depth	698.10nm

3. Results and discussion

3.1. DFT calculation study

Use The S^{2-} and HS^- components produced by Na_2S hydrolysis in the aqueous solution had a sulfidation effect on the malachite. Further, according to the diagram of pH dependent sulfide composition, sulfides mainly existed as hydrogen sulfide ions in the pH range that was most suitable for malachite flotation (pH value 7 ~ 10). Therefore, in order to better understand the actual sulfide flotation process of malachite, the adsorption mechanism of hydrogen sulfide ions on the surface of malachite (-201) was studied. Fig.1 shows the adsorption configuration of HS^- on malachite (-201), wherein Fig. 1(a) is a panoramic view of the adsorption configuration of HS^- on the surface of malachite (-201), Fig. 1(b) is the pre-adsorption HS^- , and Fig. 1(c) is the local diagram of the adsorption configuration of HS^- on the surface of malachite (-201). The numbers shown in the figures are the bond lengths between the two corresponding atoms.

From Fig. 1, it was determined that HS^- mainly adsorbs through the S and Cu atoms on the malachite (-201) surface. The S-Cu bond length is 2.26 Å, which is between the covalent radii of copper and sulphur (2.19 Å) and their ion radii (2.57 Å) (Wu et al., 2017). This indicated that strong chemical adsorption occurred between the S atom in HS^- and the Cu atom on the malachite (-201) surface. The H-S bond length of HS^- before and after adsorption changed slightly, indicating that the charge transfer caused the space structure of HS^- to spontaneously adjust during adsorption.

In Mulliken's analysis, the valence electron charges distributed around the atoms are referred to as the electron population of the atom, and the overlapping electron charge distributions between the two atoms is called the bond population. The bond population represents the strength and bonding characteristics of the ionic bond, covalent bond, or the combination of the two atoms. The structure of the HS^- adsorbed on malachite (-201) surface was optimized. The bond population between the S and Cu atoms was 0.29, which confirmed that the bond interaction between the S and Cu atoms could indeed occur. The adsorption energy ΔE_{ads} of HS^- on the malachite (-201) surface was -603.06 kJ/mol, which indicated that it could adsorb on the malachite (-201) surface. The negative adsorption energy indicated that the adsorption of HS^- on the malachite (-201) surface is a spontaneous process. The adsorption

energy ΔE_{ads} of HS^- after adsorption on the malachite (-201) surface was larger than that of S (-348.33 kJ/mol) (Wu et al., 2017), signifying that the adsorption configuration of HS^- was more stable than that of S. The interaction between HS^- and malachite was stronger than that between S^{2-} and malachite. In order to further study the sulfidation mechanism of HS^- on the malachite (-201) surface, the electronic density of states (DOS) and atomic population of each atom before and after HS^- adsorption on the malachite (-201) surface were compared and analyzed. Fig.2 shows the DOS of surface atoms before and after HS^- adsorption on the malachite (-201) surface.

Fig. 2 shows that before the adsorption of HS^- on the malachite (-201) surface, the DOS of HS^- was contributed to by S 3s, H 1s, and S 3p orbitals, whereas the near Fermi level was contributed to by the S3P orbital. The DOS of the atoms of the malachite (-201) surface changed after adsorption of HS^- on the malachite (-201) surface, and the near Fermi level was jointly contributed to by the Cu 3d, O 2p, O 2S, and S 3P orbits. In the range of 0 eV ~ -2.5 eV, the 3d orbital of Cu and the 3p orbital of S significantly overlapped, signifying that the interaction between copper and HS^- was strong. At the same time, it was found that the 2p orbital of O and the 3p orbital of S overlapped, indicating that when HS^- adsorbed on the malachite (-201) surface, in addition to reacting with Cu, it also reacted with O.

Table 2 shows the average atomic population of the system before and after HS^- adsorption on the malachite (-201) surface. It can be seen from Table 2 that the adsorption of HS^- on the malachite (-201) surface resulted in the transfer of electrons from the H atom to the Cu atom and from the HS^- atom to the S atom and O atom. After adsorption, the charge of S increased from -1.14 e to -0.21 e; the charge of the H atom in HS^- decreased from +0.14 e to +0.05 e; the charge of the Cu atom decreased from +0.93 e to +0.81 e; and the charge of the O atom decreased from -0.66 e to -0.81 e. The electrons of the C and H atoms in the malachite did not change during the sulfidation process. Unlike with the adsorption of S^{2-} on the malachite (-201) surface, the electrons of the S atom in HS^- were transferred to the Cu and O atoms after the adsorption of HS^- on the malachite (-201) surface. Furthermore, unlike during the adsorption of S^{2-} on the malachite (-201) surface, the adsorption of HS^- on the malachite (-201) surface led to an additional electron transfer from S, indicating that the reaction is more intense with a better sulfidation efficiency. These results have provided novel insight into the mechanism of sulfidation at an atomic level.

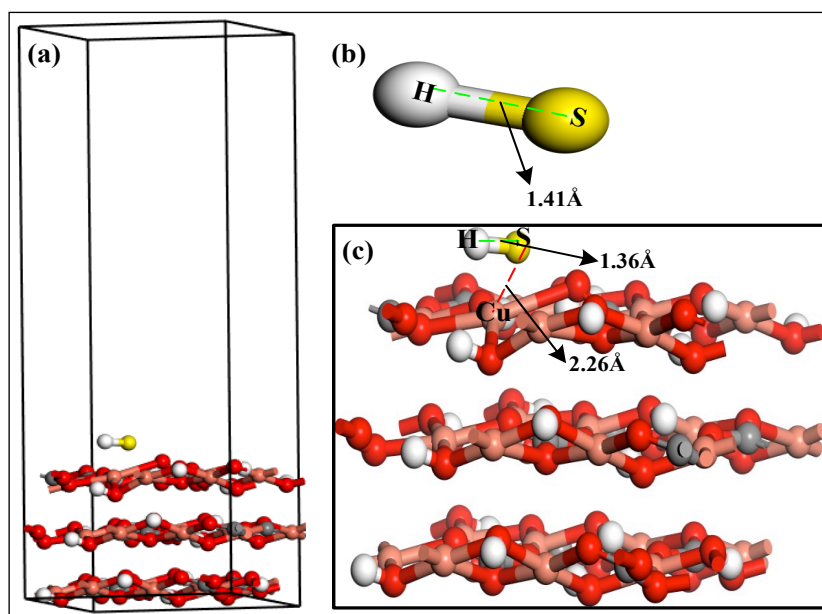


Fig. 1. Configuration of HS^- adsorption on malachite (-201) surface

3.2. TOF-SIMS study

3.2.1. Negative cumulative mass spectra of the malachite surface after sulfidation by HS^-

The negative cumulative mass spectra of the malachite surface are shown in Fig. 3. Fig. 3(a) shows that the OH^- , CO_3^- , and CuO_3H_3^- fragment ion peaks of the mass spectra were detected in the 0–150 m/z

rang of the negative cumulative spectra of the malachite surface. The existence of CuO_3H_3^- indicated that hydroxylation occurred on the malachite surface. The S^- and CuS_2^- fragment ion peaks were also detected in the same negative mass spectra segment, as shown in Fig. 3(b). This result indicated that hydrogen sulfide ions reacted with copper sites on the malachite surface.

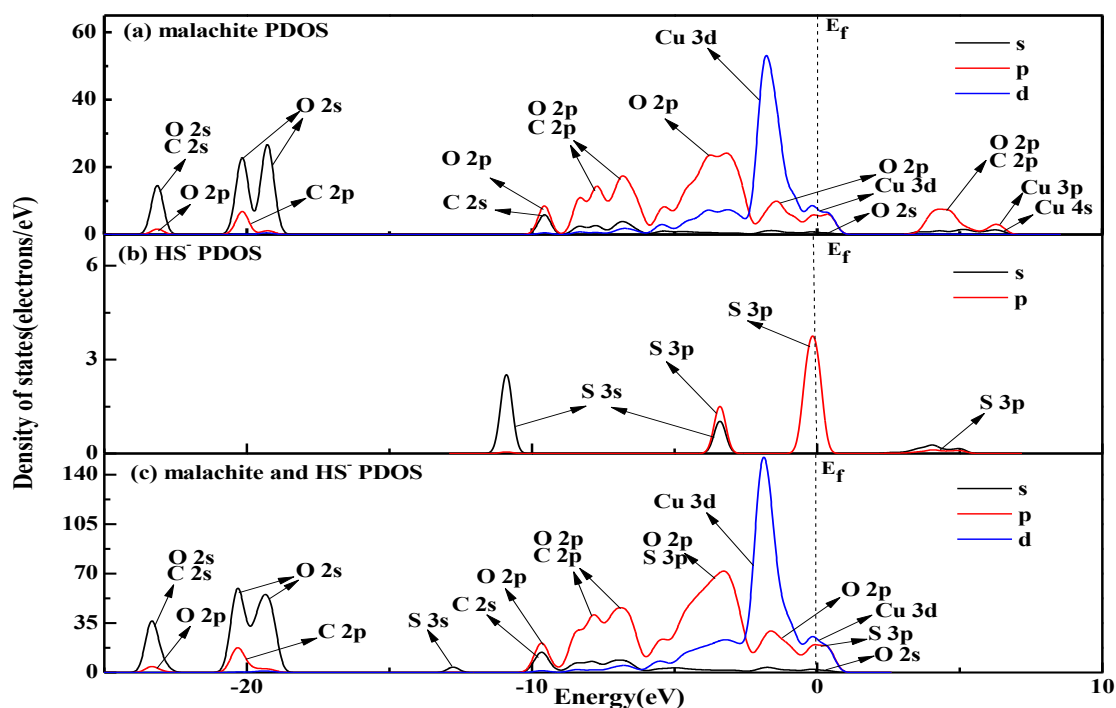


Fig. 2. PDOS of surface atom of malachite (-201) surface before and after HS^- -adsorption: (a) malachite PDOS, (b) HS^- PDOS, (c) malachite and HS^- PDOS

Table 2. Average Mulliken population of atoms before and after HS^- -adsorption on malachite (-201) surface

Absorption type	Atom Type	Atomic orbital			Total	Charge / e
		s	p	d		
Before HS^- -adsorption	C	0.88	2.42	0.00	3.30	0.70
	O	1.83	4.83	0.00	6.66	-0.66
	Cu	0.44	0.17	9.46	10.07	0.93
	$\text{H}_{\text{malachite}}$	0.63	0.00	0.00	0.63	0.38
	H_{HS^-}	0.86	0.00	0.00	0.86	0.14
After HS^- -adsorption	S	1.91	5.22	0.00	7.14	-1.14
	C	0.88	2.41	0.00	3.30	0.70
	O	1.86	4.96	0.00	6.82	-0.82
	Cu	0.49	0.17	9.53	10.19	0.81
	$\text{H}_{\text{malachite}}$	0.63	0.00	0.00	0.63	0.38
	H_{HS^-}	0.95	0.00	0.00	0.95	0.05
	S	1.91	4.32	0.00	6.21	-0.21

3.2.2. Depth profiling analysis of the malachite after sulfidation by HS^-

Fig. 4 shows that the negative ion intensities of OH^- , CO_3^- , CuO_2^- , S^- , and CuS_2^- on the sulfidized and unsulfidized malachite surfaces were a function of the depth profile. From Fig. 4(a), hydroxylation caused by malachite hydrolysis appeared to be the main reason for the differences in ion intensities of OH^- and CO_3^- along the depth profile. As can be seen in Fig. 4(b), the S^- ion intensity increased at depths of 0-5 nm, and then significantly decreased at depths of 5-75 nm. In the depth range of 0-75 nm, the CO_3^- ion intensity significantly increased. This result indicated that the HS^- was adsorbed onto the malachite surface, and that a copper sulfide film of a certain thickness was formed.

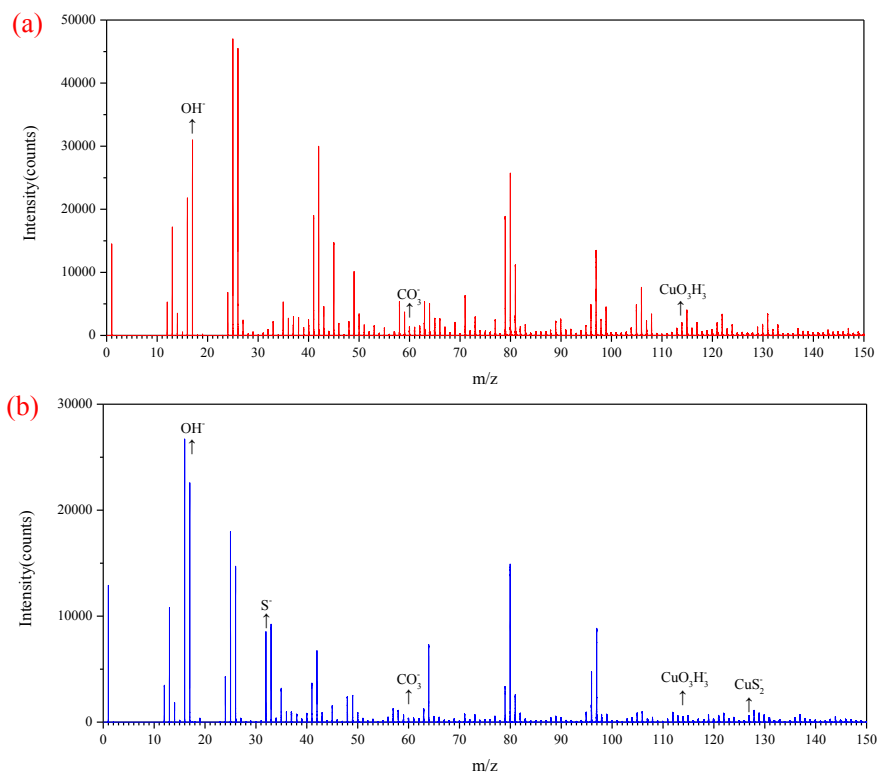


Fig. 3. Negative cumulative mass spectra at different depths: (a) malachite, (b) malachite and 1.0×10^{-3} mol/L HS^-

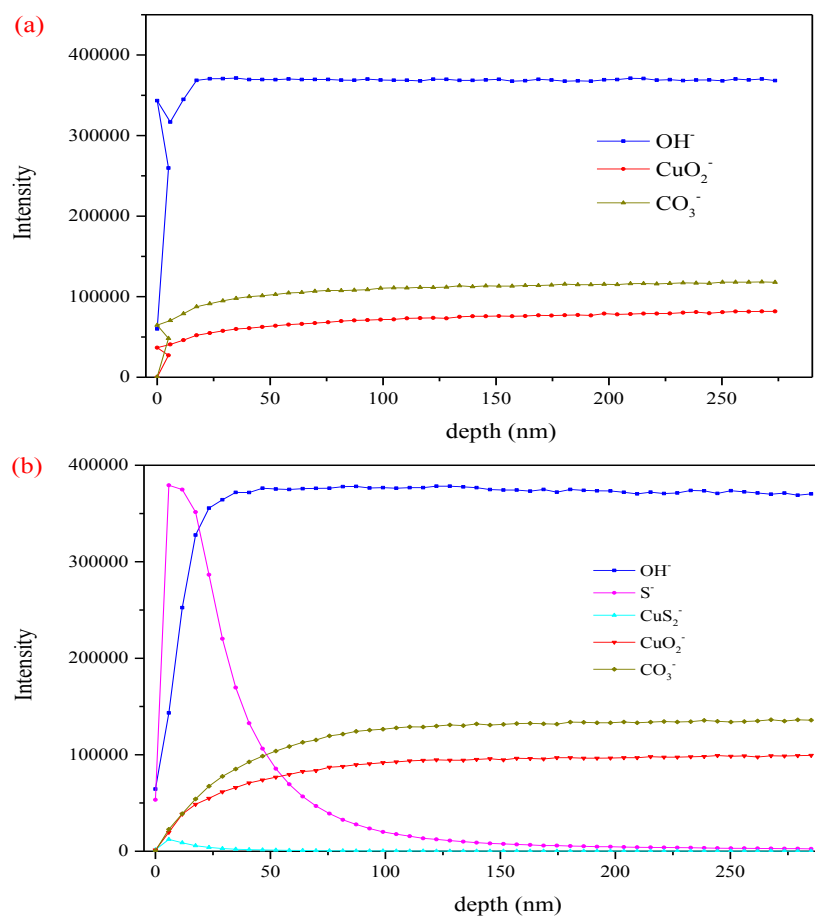


Fig. 4. Negative ion intensities depth profile of malachite surface: (a) malachite, (b) malachite and 1.0×10^{-3} mol/L HS^-

3.2.3. Sulfidation characterization using three-dimensional (3D) images

3D secondary ion images were obtained from the depth profile data (Fig. 5). The 3D images show the spatial distributions of various negative ion species on the sulfidized and unsulfidized malachite surfaces. The negative ion imaging in Fig. 5(a) shows heterogeneous distributions of OH^- , CO_3^- , and CuO_2^- on the malachite surface. After malachite sulfidation with HS^- (Fig. 5(b)), the S^- negative ion thickness on the malachite surface was significantly increased. The surface thickness of CO_3^- and CuO_2^- revealed a few vacancies when malachite was sulfidized by HS^- . These vacancies indicated that the HS^- reacted with OH^- and CO_3^- groups on the malachite surface, forming a copper sulfide film.

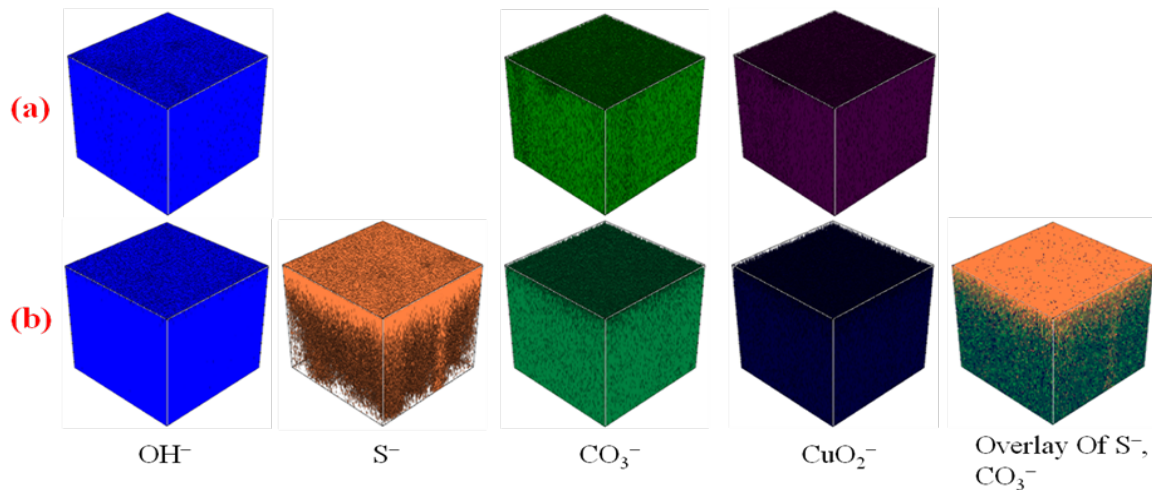


Fig. 5. 3D negative ion images from depth profile of malachite in $100\ \mu\text{m} \times 100\ \mu\text{m}$: (a) malachite, (b) malachite and $1.0 \times 10^{-3}\ \text{mol/L HS}^-$

4. Conclusions

This study utilized DFT calculations and TOF-SIMS to investigate the mechanisms by which the sulfidation of malachite by hydrogen sulfide ions occurs. The DFT calculations indicated that the adsorption configuration of HS^- is more stable than that of S^- , and the interaction between HS^- and malachite is stronger than that between S^- and malachite, due to the higher number of electron transfers in the solution which accelerate the sulfidation reaction rate. The DOS of the atoms on the surface of the malachite (-201) after adsorption of HS^- revealed that the near Fermi level is jointly contributed to by the Cu 3d, O 2p, O 2s, and S 3p orbitals. In the range of $0 \sim -2.5\ \text{eV}$, the interaction between copper and HS^- is strong. It was found that the 2p orbital of O and the 3p orbital of S overlapped, demonstrating that when HS^- adsorbed on the malachite (-201) surface, it not only reacted with Cu, but also with O. The TOF-SIMS analysis showed strong evidence that the copper sulfide film on the malachite surface increased with the addition of HS^- , S^- and CuS_2^- , and that their fragment ion peaks were detected in the $0-150\ \text{m/z}$ negative segment of the mass spectra.

Acknowledgments

This research project was supported by the National Natural Science Foundation of China (51964024) and Yunnan Provincial Department of Education Science Research Fund Project (2018JS031).

References

- BESSIERE, J., HOUSNI, A.E., PREDALI, J.J., 1991. Dielectric study of activation and deactivation of malachite by sulfide ions. *Int. J. Min. Process.* 33, 165-183.
- CAO, Z.F., ZHONG, H., LIU, G.Y., ZHAO, S.J., 2009. Techniques of copper recovery from Mexican copper oxide ore. *Min. Sci. Techno.* 19, 45-48.
- CASTRO, S., SOTO, H., GOLDFARB, J., LASKOWSKI, J., 1974a. Sulfidizing reactions in the flotation of oxidized copper mineral, I. Chemical factors in the sulfidization of copper mineral. *Int. J. Miner. Process.* 1, 141-149.

- CASTRO, S., SOTO, H., GOLDFARB, J., LASKOWSKI, J., 1974b. *Sulphidizing reactions in the flotation of oxidized copper minerals, II. Role of the adsorption and oxidation of sodium sulphide in the flotation of chrysocolla and malachite*. Int. J. Miner. Process. 1, 151-161.
- CHEN, Y., LIU, M., CHEN, J.H., LI, Y.Q., ZHAO, C.H., MU, X., 2018. *A density functional based tight binding (DFTB plus) study on the sulfidization-amine flotation mechanism of smithsonite*. Appl. Surf. Sci. 458, 454-463.
- CLARK, S.J., SEGALL, M.D., PICKARD, C.J., HASNIP, P.J., PROBERT, M.I.J., REFSON, K., PAYNE, M.C., 2005. *First principles methods using CASTEP*. Z. Kristallogr. 220, 567-570.
- CORIN, K.C., KALICHINI, M., O'CONNOR, C.T., SIMUKANGA, S., 2017. *The recovery of oxide copper minerals from a complex copper ore by sulphidisation*. Min. Eng. 102, 15-17.
- EJTEMAEI, M., GHARABAGHI, M., IRANNAJAD, M., 2014. *A review of zinc oxide mineral beneficiation using flotation method*. Adv. Colloid. Interfac. 206, 68-78.
- FENG, Q.C., ZHAO, W.J., WEN, S.M., CAO, Q.B., 2017. *Copper sulfide species formed on malachite surfaces in relation to flotation*. J. Ind. Eng. Chem. 48, 125-132.
- FENG, Q.C., ZHAO, W.J., WEN, S.M., 2018a. *Ammonia modification for enhancing adsorption of sulfide species onto malachite surfaces and implications for flotation*. J. Alloy. Compd. 744, 301-309.
- FENG, Q.C., ZHAO, W.J., WEN, S.M., 2018b. *Surface modification of malachite with ethanediamine and its effect on sulfidization flotation*. Appl. Surf. Sci. 436, 823-831.
- GUSH, J.C.D., 2005. *Flotation of oxide minerals by sulphidization-the development of a sulphidization control system for laboratory testwork*. J. S. Afr. Inst. Min. Metall. 105, 193-197.
- HUANG, Y.G., NIU, X.X., LIU, G.Y., LIU, J., 2019. *Novel chelating surfactant 5-heptyl-1,2,4-triazole-3-thione: Its synthesis and flotation separation of malachite against quartz and calcite*. Min. Eng. 131, 342-352.
- KALICHINI, M., CORIN, K.C., O'CONNOR, C.T., SIMUKANGA, S., 2017. *The role of pulp potential and the sulphidization technique in the recovery of sulphide and oxide copper minerals from a complex ore*. J. S. Afr. Inst. Min. Metall. 117, 803-810.
- KONGOLO, K., KIPOKA, M., MINANGA, K., MPOYO, M., 2003. *Improving the efficiency of oxide copper-cobalt ores flotation by combination of sulphidisers*. Miner. Eng. 16, 1023-1026.
- LAI, H., DENG, J.S., LIU, Q.J., WEN, S.M., SONG, Q., 2021. *Surface chemistry investigation of froth flotation products of lead-zinc sulfide ore using ToF-SIMS and multivariate analysis*. Sep. Purif. Technol. 254, 117655.
- LEE, K., ARCHIBALD, D., MCLEAN, J., REUTER, M.A., 2009. *Flotation of mixed copper oxide and sulphide minerals with xanthate and hydroxamate collectors*. Min. Eng. 22, 395-401.
- LEE, J.S., NAGARAJ, D.R., COE, J.E., 1998. *Practical aspects of oxide copper recovery with alkylhydroxamates*. Miner. Eng. 10, 929-939.
- LI, L.Q., ZHAO, J.H., XIAO, Y.Y., HUANG, Z.Q., GUO, Z.Z., LI, F.X., DENG, L.Q., 2019. *Flotation performance and adsorption mechanism of malachite with tert-butylsalicylaldoxime*. Sep. Purif. Technol. 210, 843-849.
- LIU, G.Y., HUANG, Y.G., QU, X.Y., XIAO, J.J., YANG, X.L., XU, Z.H., 2016. *Understanding the hydrophobic mechanism of 3-hexyl-4-amino-1,2,4-triazole-5-thione to malachite by TOF-SIMS, XPS, FTIR, contact angle, zeta potential and micro-flotation*. Colloid. Surface. A. 503, 34-42.
- LIU, C., ZHU, G.L., SONG, S.X., LI, H.Q., 2018. *Interaction of gangue minerals with malachite and implications for the sulfidization flotation of malachite*. Colloid. Surface. A. 555, 679-684.
- LIU, C., SONG, S.X., LI, H.Q., LI, Y.B., AI, G.H., 2019. *Elimination of the adverse effect of calcite slimes on the sulfidization flotation of malachite in the presence of water glass*. Colloid. Surface. A. 563, 324-329.
- MALGHAN, S.G., 1986. *Role of sodium sulfide in the flotation of oxidized copper, lead, and zinc ores*. Min. Metall. Process. 3, 158-163.
- MARION, C., JORDENS, A., LI, R.H., RUDOLPH, M., WATERS, K.E., 2017. *An evaluation of hydroxamate collectors for malachite flotation*. Sep. Purif. Technol. 183, 258-269.
- PARK, K., PARK, S., CHOI, J., KIM, G., TONG, M., KIM, H., 2016. *Influence of excess sulfide ions on the malachite-bubble interaction in the presence of thiol-collector*. Sep. Purif. Technol. 168, 1-7.
- PERDEW, J.P., BURKE, K., ERNZERHOF, M., 1996. *Generalized gradient approximation made simple*. Phys. Rev. Lett. 77(18), 3865-3868.
- PERDEW, J.P., CHEVARY, J.A., VOSKO, S.H., JACKSON, K.A., PEDERSON, M.R., SINGH, D.J., FIOLETTI, C., 1992. *Atoms, molecules, solids, and surfaces: Applications of the generalized gradient approximation for exchange and correlation*. Phys. Rev. B. 46, 6671-6687.

- PERDEW, J.P., WANG, Y., 1992. *Accurate and simple analytic representation of the electron-gas correlation energy*. Phys. Rev. B. 45, 13244-13249.
- PERDEW, J.P., YUE, W., 1986. *Accurate and simple density functional for the electronic exchange energy: Generalized gradient approximation*. Phys. Rev. B. 33(12), 8800-8802.
- SHEN, P.L., LIU, D.W., ZHANG, X.L., JIA, X.D., SONG, K.W., LIU, D., 2019. *Effect of $(\text{NH}_4)_2\text{SO}_4$ on eliminating the depression of excess sulfide ions in the sulfidization flotation of malachite*. Min. Eng. 137, 43-52.
- WU, D.D., MAO, Y.B., DENG, J.S., WEN, S.M., 2017. *Activation mechanism of ammonium ions on sulfidation of malachite (-201) surface by DFT study*. Appl. Surf. Sci. 410, 126-133.
- YIN, W.Z., SUN, Q.Y., LI, D., TANG, Y., FU, Y.F., YAO, J., 2019. *Mechanism and application on sulphidizing flotation of copper oxide with combined collectors*. T. Nonferr. Metal. Soc. 29, 178-185.
- ZHOU, R., CHANDER, S., 1993. *Kinetics of sulfidization of malachite in hydrosulfide and tetrasulfide solutions*. Int. J. Miner. Process. 37, 257-272.